Journal of Creativity Student
http://journal.unnes.ac.id/journals/jcs

Evaluation of Gelatin Concentration Variations on the Porosity of Green Mussel Shell Hydroxyapatite Scaffolds

Firda Aulia Rahman[1]*, Widi Widayat[2]

[1,2]*Department of Mechanical Engineering, Universitas Negeri Semarang, Indonesia*

*Corresponding Author: firdaauliarahman3@students.unnes.ac.id

Abstract
The increasing demand for scaffolds in orthopedic applications has driven research into locally sourced biomaterials. This study evaluates the effect of varying gelatin concentrations (2%, 3%, and 4% w/w) on the porosity of hydroxyapatite (HA) scaffolds synthesized from green mussel shells (*Perna viridis*). HA was synthesized through a calcination process at a temperature of 900°C, followed by microwave-assisted ultrasonic precipitation, yielding a phase purity of 98.4% as confirmed by X-ray diffraction (XRD). The composite scaffolds were fabricated by mixing HA with type B gelatin at three concentrations, molded into cylindrical molds (6 mm diameter × 6 mm height), and dried at 40°C for 24 hours. Porosity was measured using the Archimedes liquid displacement method with 96% ethanol. The results indicated porosity values of 57.4% ± 1.68%, 60.2% ± 2.97%, and 58.1% ± 1.15% for gelatin concentrations of 2%, 3%, and 4%, respectively. All formulations exceeded the lower limit of commercial scaffold porosity standards (35–50%), with the 4% formulation approaching the upper limit of that range. This study demonstrates that HA derived from green mussel shells combined with gelatin produces scaffolds with a porosity comparable to commercial products, thereby offering an economical and sustainable alternative for bone tissue engineering applications.

Keywords: gelatin, green mussel shells, hydroxyapatite, porosity, scaffold

INTRODUCTION

The demand for scaffold substitute materials in dentistry and orthopedics continues to increase along with the rising number of bone implant procedures. Most scaffold products available in the market still rely on imports and are relatively expensive, leading to increased medical costs and vulnerability to global supply fluctuations (Zhao et al., 2021). Therefore, the development of locally sourced, economical, and easily manufacturable scaffolds that meet biomedical standards is highly needed. Green mussel shells (*Perna viridis*) are an abundant organic waste found around fishponds and seafood restaurants. These shells contain a high level of calcium carbonate ($CaCO_3$), which has the potential to be converted into hydroxyapatite (HA) through thermal or chemical processes (Charlena et al., 2022; Dugaich et al., 2025). HA is the primary mineral component of human bone, possessing bioactive, biocompatible, and osteoconductive properties, making it highly relevant as a scaffold base material (Pratama et al., 2025).

Various previous studies have demonstrated that biomineral waste can be synthesized into HA (Arokiasamy et al., 2022). A study conducted by Dugaich et al. (2025) using the wet chemical precipitation method successfully synthesized HA from *P. viridis* shells, yielding pure HA with a Ca/P ratio approaching 1.67. However, that study focused on crystalline phase characterization without the addition of a pore-forming agent, resulting in low porosity (below 40%). On the other hand, Wu et al. (2024) investigated HA-gelatin composites using the freeze-drying method and proved that gelatin enhanced osteoblast viability (Ismail et al., 2022). A study by Jiao et al. (2023) also evaluated the relationship between porosity and the compressive strength of ceramic scaffolds; however, the

materials used were synthetic.Based on the comparison of these previous findings, scaffolds made from pure HA powder tend to exhibit high density and low porosity, which hinders osteoblast migration, nutrient diffusion, and vascularization. To overcome these limitations, a natural polymer such as gelatin was incorporated. Gelatin was selected because it is a collagen derivative that has been proven to improve biological properties, accelerate tissue integration, and support bone regeneration (Naghavi et al., 2022). In a composite system, gelatin plays a role in binding HA particles through hydrogen and electrostatic bonds, as well as modulating interparticle cavities during the compaction process (Lukin et al., 2023). Furthermore, a study by Priyani et al. (2025) demonstrated that HA synthesis from green mussel shells using an ultrasonic-assisted microwave method was capable of yielding high purity (98.5%) with a crystallite size of 8.68 nm.

Recent studies on composite scaffolds indicate that the combination of bioceramics and natural polymers produces scaffolds with superior physical and biological characteristics. Guagnini et al. (2024) developed an alginate/hydroxyapatite composite scaffold reinforced with BGMS10 bioactive glass, which yielded a porosity ranging from 70.2% to 84.6% depending on the bioactive glass concentration. However, excessively high porosity can reduce the mechanical strength of the scaffold. Daskalakis et al. (2024) reported that the GreenBone scaffold derived from the biomorphic transformation of rattan wood possessed a volume porosity of 57% with a compressive strength of 10.18 MPa, which is equivalent to natural trabecular bone. Shan et al. (2025) evaluated 3D-printed HA-PLA scaffolds with two infill density levels (50% and 70%) and discovered that the scaffold with higher porosity (HA-PLA50) exhibited higher expression of the osteogenic gene COL1A1. González-Henríquez et al. (2022) fabricated multi-hierarchical PCL/nHA/NaCl-based scaffolds with a global porosity of approximately 42% through a combination of 3D printing and salt leaching. Meanwhile, Kang et al. (2021) reviewed various strategies for integrating bioactive vesicles into scaffolds for bone regeneration, emphasizing the importance of an interconnected pore structure for cell migration and nutrient transport.

The specimens used in this study were composite scaffolds consisting of HA synthesized from green mussel shells mixed with type B gelatin at varying concentrations of 2%, 3%, and 4% (w/w). The specimens were cylindrical in shape with a diameter of 6 mm and a height of 6 mm. The scaffold porosity was subsequently measured and compared with reference data of commercial products (35–50%) (Chinnasami et al., 2023; Gregor et al., 2017) as well as with literature variant composite scaffold data. The novelty of this research lies in the integrated utilization of local green mussel shell waste with variations in gelatin and HA concentrations (Akbari & Khazaeinejad, 2025; Zhao et al., 2021). The objective of this study is to evaluate the effect of varying gelatin concentrations (2%, 3%, and 4%) on the porosity of HA-gelatin composite scaffolds derived from green mussel shells.

METHOD

The materials used included green mussel shell (GMS) powder as the calcium source, diammonium hydrogen phosphate (≥99%) as the phosphate source, type B gelatin as the polymer matrix, distilled water as the solvent, and 96% ethanol as the density measurement medium. The primary equipment used included a box muffle furnace for the calcination process, a microwave for hydroxyapatite synthesis, a sonicator, an oven for drying the scaffolds, an X-ray diffractometer (XRD) for crystalline phase characterization, and an analytical balance with a precision of 0.001 grams for mass measurements. The initial raw material, consisting of whole green mussel shells, was cleaned of adhering impurities and subsequently dried. The dried shells were crushed into smaller pieces and then ground into powder using a disc mill. The resulting powder was sieved using a 100-mesh sieve to obtain a more uniform particle size prior to the calcination stage.

The GMS powder was poured into a porcelain crucible, placed inside the box muffle furnace at room temperature, and the furnace was tightly sealed. The equipment was gradually heated to 600°C and held stable for 1 hour. Subsequently, the temperature was gradually increased to 900°C and held stable for 5 hours. This process converted $CaCO_3$ into CaO (Fitriyana et al., 2024). After 5 hours, the temperature was gradually decreased without opening the box muffle furnace. The porcelain crucible was removed once the calcined product had reached room temperature. The calcined product was weighed using a digital balance with a precision of 0.001 grams to determine material shrinkage during the calcination process. The materials were measured using a digital balance. Diammonium hydrogen phosphate was dissolved in distilled water in a measuring cylinder, then placed in a sonicator partially filled with water for 10 minutes at a power of 600 W. Next, the calcined GMS was dissolved in distilled

water, and the measuring cylinder containing the shell solution was placed in the sonicator for 20 minutes at 600 W. The diammonium hydrogen phosphate solution was gradually added to the GMS solution while the sonication process was ongoing until completion (Fitriyana et al., 2024; Prasetyo et al., 2025; Priyani et al., 2025).

Subsequently, the measuring cylinder containing the mixed solution was placed in a microwave and heated at medium power for 3 minutes. The solution was stored until it reached room temperature. The mixed solution was soaked in 1 liter of distilled water for 30 minutes, and the soaking water was then discarded. The soaking was repeated using 1 liter of distilled water for 15 minutes, and the water was subsequently discarded. This washing process was repeated 3 times. The solution was filtered using filter paper clamped to a container until the water content was reduced, leaving a precipitate. The precipitate was dried in an oven at 110°C for 60 minutes. The heating was repeated if the precipitate remained wet. The dried product was crushed using a mortar to break up any agglomerations (Prasetyo et al., 2025; Priyani et al., 2025).

Scaffolds were fabricated by mixing the synthesized HA from GMS and gelatin according to predetermined concentrations, namely 2%, 3%, and 4% (w/w). 5 mL of distilled water was added to obtain a homogeneous mixture. The mixture was then stirred using a magnetic stirrer at 60°C for 10 minutes until a homogeneous slurry was formed. The obtained slurry was poured into cylindrical silicone molds with a diameter of 6 mm and a height of 6 mm. The molding process using silicone molds aimed to produce scaffolds with uniform dimensions. Subsequently, the scaffolds were dried in an oven at 40°C for 24 hours.

Table 1. Scaffold Composition

Specimen	Ratio (%)	Gelatin (gr)	HA (gr)
G-HA-2	2:98	0,08	3,92
G-HA-3	3:97	0,12	3,88
G-HA-4	4:96	0,16	3,84

Total porosity measurement was conducted using the fluid displacement (Archimedes) method based on 96% ethanol to prevent the specimens from dissolving. The samples were weighed in a dry state to obtain the dry weight (W_1), soaked for 12 minutes until saturated to obtain the saturated weight (W_2), and weighed while suspended in the liquid to obtain the suspended weight (W_3) (Maji et al., 2015; Nawafi et al., 2022). The weight-based liquid displacement method was used for porosity measurement because it is more accurate and precise than volume-based measurements. The porosity value was calculated using the equation:

$$Porosity(\%) = \frac{W_2 - W_1}{W_2 - W_3} \times 100$$

Data validity was ensured through internal validity referencing the international standards ASTM C373 and ISO 18754, as well as routine calibration of the analytical balance. Data reliability was achieved by replicating the test three times for each variant and calculating the average and standard deviation (SD). Data analysis was conducted quantitatively and descriptively by comparing the average porosity values of the samples against commercial porosity references (35–50%, with a midpoint of 42% or 43%) (Zhao et al., 2021) as well as against composite scaffold porosity data from current literature.

Data analysis was conducted quantitatively and descriptively. The porosity data were presented in the form of averages and standard deviations. Comparisons were made among the three gelatin concentration variants and against commercial scaffold porosity standard references as well as composite scaffolds from the literature. Data interpretation was based on the Gibson-Ashby cellular solid theory, the void-filling mechanism by the polymer matrix, and the influence of slurry characteristics on the scaffold's pore structure (Zhao et al., 2021).

RESULTS AND DISCUSSION

The XRD characterization results indicated that the synthesized hydroxyapatite had a phase content of 98.4%, while the identified minor phases were calcite ($CaCO_3$) at 1.3% and portlandite ($Ca(OH)_2$) at 0.3%. The dominance of hydroxyapatite demonstrated that the synthesis method used successfully produced hydroxyapatite with a high purity level. The high percentage of hydroxyapatite indicated that the majority of the calcium carbonate from the green mussel shells (GMS) had been

successfully converted into hydroxyapatite. The presence of calcite and portlandite in minute amounts indicated that there were still slight residual phases from the reaction or hydration products during the synthesis process (Fitriyana et al., 2024; Prasetyo et al., 2025; Priyani et al., 2025). However, the amounts of both phases were relatively low, thus not diminishing the dominance of the generated hydroxyapatite phase. These results are in line with the study by Priyani et al. (2025), which reported that hydroxyapatite synthesis from biomineral waste using microwave and ultrasonic assistance was capable of producing a dominant hydroxyapatite phase (98.4%) with relatively small impurities. Ultrasonic mixing proved effective in improving solution homogeneity, thereby accelerating the HA formation reaction and preventing particle agglomeration (Fitriyana et al., 2024).

The high HA purity (98.4%) achieved in this study ensured that the generated scaffolds possessed optimal bioactivity. Daskalakis et al. (2024) demonstrated that high-purity HA scaffolds were capable of supporting osteoblast cell viability above 90% without cytotoxic effects. Furthermore, Guagnini et al. (2024) proved that the addition of bioactive components into a polymer matrix did not interfere with scaffold biocompatibility, but rather enhanced cell proliferation. This supports the premise that HA-gelatin composites derived from green mussel shells have immense potential as bone regeneration scaffolds.

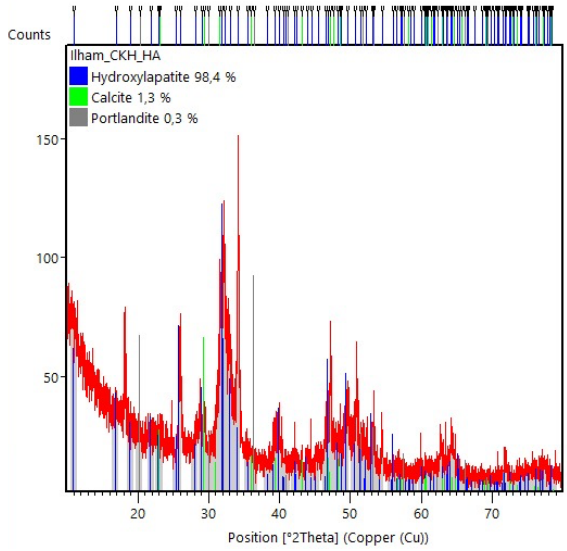

Figure 1. XRD diffractogram of GMS HA

Gelatin as the organic phase acted as a binding matrix that united the HA particles and created a cohesive three-dimensional structure. Gelatin is a collagen denaturation product containing the RGD (Arg-Gly-Asp) amino acid sequence, which is a recognition ligand for integrins on the surface of osteoblast cells (Wu et al., 2024). This facilitates better cell adhesion compared to pure HA scaffolds. Interfacial interactions between HA and gelatin occurred through hydrogen bonds between the carbonyl and amine groups of gelatin and the hydroxyl and phosphate groups of HA. In addition, electrostatic interactions between positive charges on the gelatin surface (at a pH below its isoelectric point) and negative charges on the HA surface created stable bonds (Lukin et al., 2023). These interactions not only strengthened the structural integrity of the scaffold but also created a surface topography that supported cell spreading. During the fabrication process, the water-soluble gelatin filled the interparticle spaces of HA. As the drying process proceeded, the water evaporated and the gelatin matrix hardened, binding the HA particles more compactly. This mechanism created an interconnected pore network, which is essential for the transport of nutrients, oxygen, and cellular waste products during the bone regeneration process (Kang et al., 2021). An interconnected pore structure also facilitates vascularization, which is a crucial prerequisite for successful bone regeneration.

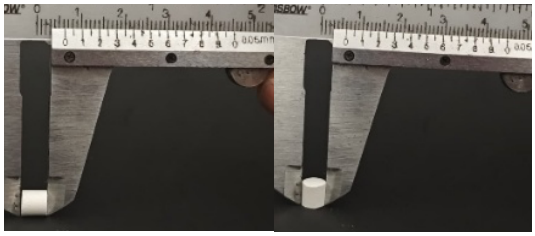

Figure 2. Scaffold results

Table 2. Detailed Data of Scaffold Porosity Measurements

Specimen (Gelatin:HA)	Weight (gr)
2%:98%	0,127
	0,151
	0,160
3%:97%	0,134
	0,137
	0,142
4%:96%	0,129
	0,141
	0,142

The increase in gelatin concentration affected the scaffold structure. During the drying process, water evaporation left small cavities within the scaffold matrix, thereby forming unintentionally designed pores. Thus, the generated porosity was influenced not only by the material composition but also by the slurry characteristics during the fabrication process. This indicates that slurry control is a crucial factor in producing scaffolds with uniform shapes and more stable structures (Peng et al., 2023).

Table 3. Scaffold Porosity

Specimen (Gelatin:HA)	Mean (%)	Standard Deviation
2%:98%	57,4%	1,68%
3%:97%	60,2%	2,97%
4%:96%	58,1%	1,15%

The porosity data exhibited a non-linear pattern. At a 2% gelatin concentration, the average porosity was 57.4%. Increasing the gelatin concentration to 3% actually increased the porosity to 60.2%. However, at a 4% concentration, the porosity decreased again to 58.1%. This pattern is interesting to analyze further. The void-filling mechanism by gelatin occurred because the water-soluble gelatin filled the spaces between the HA particles. As the drying process progressed, the water evaporated and the gelatin matrix hardened, binding the HA particles more compactly and sealing the microscopic gaps between them (Sun et al., 2025). At concentrations of 2% to 4%, the scaffold porosity remained relatively high (above 56%) because the amount of polymer matrix was not yet sufficient to fill all interparticle voids. This is in accordance with the Gibson-Ashby cellular solid theory, where an increase in the solid fraction (binding matrix) will reduce the total porosity fraction (Tseng et al., 2024). At a 2% concentration, the amount of available gelatin was relatively small to fill all HA interparticle spaces. The generated slurry had a low viscosity, resulting in an uneven gelatin distribution and many unfilled voids. During drying, water evaporation from the dilute slurry left larger and more numerous pore channels, thereby producing a considerably high porosity (57.4%). However, due to the low gelatin content, the structural integrity of the scaffold became less optimal, which was evident from the presence of shrinkage and dimensional instability.

At a 3% concentration, the increased amount of gelatin caused the slurry to become more viscous, yet still fluid enough to be poured into the molds. This increased viscosity led to a more heterogeneous distribution of gelatin within the HA matrix. During drying, the water trapped inside the more viscous gelatin matrix evaporated and left larger and more interconnected pore channels compared to the 2% concentration. This caused the porosity to increase to 60.2%. However, there was a high standard deviation (2.97%) at this concentration, indicating an instability in the fabrication process or uneven pore distribution due to the slurry's viscosity becoming thicker and difficult to mold

manually (Zhao et al., 2021). At a 4% concentration, a further increase in the amount of gelatin caused the slurry to become highly viscous. The denser gelatin matrix began to fill the HA interparticle voids more effectively, thereby reducing the number of pores formed from water evaporation. Furthermore, the contraction of the gelatin matrix during drying sealed some previously open pores. Consequently, the porosity decreased to 58.1%.

This decrease in porosity indicated that the void-filling effect by gelatin began to dominate over the pore-forming effect from water evaporation. This is consistent with the Gibson-Ashby theory, which states that an increase in the binder matrix fraction will reduce the total porosity fraction (Tseng et al., 2024). Additionally, the lower standard deviation (1.15%) indicated that the pore distribution at the 4% concentration was more homogeneous compared to the 3% concentration. To evaluate the feasibility of the HA-gelatin scaffolds derived from green mussel shells, a comparison was made against commercial scaffolds and composite scaffolds from recent studies. The porosity range of commercial scaffolds for bone regeneration is typically between 35% and 50% (Chinnasami et al., 2023; Gregor et al., 2017). However, several commercial and composite scaffolds from the literature possess a broader porosity range.

Table 4. Comparison of Porosity Across Various Scaffolds

Scaffold Type	Material	Porosity (%)
Commercial Scaffold (Chinnasami et al., 2023)	β-TCP/HA	35–50
GreenBone (commercial) (Daskalakis et al., 2024)	HA/β-TCP from rattan	57
Kasios (commercial) (Daskalakis et al., 2024)	HA/β-TCP	64 ± 4
Engipore (commercial) (Daskalakis et al., 2024)	HA	~60
Alg/Hap (Guagnini et al., 2024)	Alginate/HAp	84,6 ± 0,3
Alg/HAp-BGMS10 6% (Guagnini et al., 2024)	Alginate/HAp/Bioglass	80,2 ± 1,1
Alg/HAp-BGMS10 12% (Guagnini et al., 2024)	Alginate/HAp/Bioglass	70,2 ± 0,6
HA-PLA50 (Shan et al., 2025)	HA/PLA 3D-printed	~50
HA-PLA70 (Shan et al., 2025)	HA/PLA 3D-printed	~30
PCL/nHA/NaCl (González-Henríquez et al., 2022)	PCL/nHA 3D-printed	42,08 ± 4,78
Collagen-HA scaffold (Kang et al., 2021)	*Collagen-HA*	50–70
G-HA-2	HA CKH/Gelatin 2%	57,4 ± 1,68
G-HA-3	HA CKH/Gelatin 3%	60,2 ± 2,97
G-HA-4	HA CKH/Gelatin 4%	58,1 ± 1,15

Based on Table 4, the green mussel shell HA-gelatin scaffolds developed in this study exhibited porosities (57.4–60.2%) that were above the target range of conventional commercial scaffolds (35–50%) yet were equivalent to or even lower than some commercial and composite scaffolds from the literature. The GreenBone scaffold, which is a CE-marked commercial product, possesses a porosity of 57% (Daskalakis et al., 2024), which is very close to the porosity of G-HA-2 (57.4%) in this study. This demonstrates that green mussel shell waste-based scaffolds have a porosity potential equivalent to commercial products already available on the market.

The alginate/HAp composite scaffolds developed by Guagnini et al. (2024) possessed a significantly higher porosity (70.2–84.6%) compared to the scaffolds in this study. This difference was caused by the different fabrication methods, where Guagnini et al. (2024) utilized the freeze-drying technique, which produces larger and more interconnected pores. Meanwhile, Shan et al. (2025) employed a 3D printing technique to fabricate HA-PLA scaffolds with infill levels of 50% and 70%, resulting in more controlled porosity but with a different range. González-Henríquez et al. (2022) reported a global porosity of 42.08% for PCL/nHA/NaCl scaffolds fabricated through a combination of 3D printing and salt leaching, which falls below the porosity range of the scaffolds in this study.

Kang et al. (2021), in their review, mentioned that collagen-HA scaffolds commonly used in bone tissue engineering exhibit porosities ranging from 50% to 70%, which encompasses the porosity range of the HA-gelatin scaffolds in this study. This confirms that the porosity of the scaffolds developed in this study falls within a relevant range for bone regeneration applications. Daskalakis et al. (2024) also reported that the GreenBone scaffold with a porosity of 57% was capable of supporting the viability of G292 osteoblast cells above 90% without cytotoxic effects, and the cells were able to migrate into the pores to a depth of 300 μm. Considering that the scaffolds in this study exhibited an equivalent porosity (57.4–60.2%), it can be expected that the green mussel shell HA-gelatin scaffolds would also

be capable of optimally supporting osteoblast cell proliferation and migration. Additionally, Shan et al. (2025) demonstrated that HA-PLA scaffolds with a higher porosity (HA-PLA50) produced higher expression of the COL1A1 osteogenic gene compared to scaffolds with a lower porosity (HA-PLA70), supporting the importance of adequate porosity for osteogenic differentiation.

Guagnini et al. (2024) found that increasing the bioactive glass content in alginate/HAp scaffolds decreased the porosity from 84.6% to 70.2%, yet actually increased MG-63 cell proliferation. This indicates that a higher porosity does not always result in better biological performance, and a balance between porosity and material composition is highly important. In this context, the HA-gelatin scaffolds in this study, with a porosity of 57–60%, can be considered to fall within an optimal range that balances the need for pore space for cell migration with the structural integrity of the scaffold.

González-Henríquez et al. (2022) reported that PCL/nHA/NaCl scaffolds with a global porosity of 42% were capable of supporting MC3T3 cell viability equivalent to the control, with a significant increase when coated with a functional hydrogel. This indicates that even scaffolds with a porosity lower than those generated in this study can still support cell proliferation, meaning that HA-gelatin scaffolds with a porosity of 57–60% hold highly promising biological potential. Based on these comparisons, it can be concluded that the G-HA-4 formulation with a porosity of 58.1% is the formulation closest to the commercial reference midpoint (43%) with better dimensional stability (lowest standard deviation: 1.15%). However, all formulations have entered or exceeded the commercial target porosity range, proving that local green mussel shell waste materials combined with type B gelatin are capable of simulating the macroscopic physical properties of commercial scaffold products. Further validation regarding pore interconnectivity, mechanical testing, and in vitro biological assays needs to be conducted to ensure clinical feasibility; nonetheless, based on basic porosity parameters, this local waste material has demonstrated highly promising potential.

CONCLUSION

Based on the results and discussion, it can be concluded that an increase in gelatin concentration does not linearly decrease the porosity of hydroxyapatite (HA) scaffolds derived from green mussel shells. The XRD characterization results verified that the local synthetic HA possessed high purity (98.4%), confirming the success of the synthesis and the validity of using green mussel shells as a biomaterial source. The success of the HA-gelatin composite scaffolds was achieved through the synergy between the osteoconductive bioactive properties of HA and the capability of gelatin as a binding matrix that provides cell adhesion sites, creating an interconnected pore structure essential for bone regeneration. Archimedes measurements demonstrated that the scaffold porosity ranged from 57.4% to 60.2%, which overall has entered or exceeded the commercial scaffold porosity reference standard (35–50%) and is equivalent to the commercial product GreenBone (57%). The porosity pattern that increased from a 2% concentration (57.4%) to 3% (60.2%) and subsequently decreased at a 4% concentration (58.1%) is explained by two competing mechanisms. At 2% to 3% concentrations, porosity increased because the still-low slurry viscosity caused an uneven gelatin distribution, and water evaporation during drying left larger and more interconnected pore channels. At 3% to 4% concentrations, porosity decreased because the increased amount of gelatin caused the slurry to become more viscous, allowing the gelatin matrix to fill the HA interparticle voids more effectively, while the matrix contraction during drying sealed some of the previously open pores. The 4% (w/w) formulation was considered the most optimal as it possessed a porosity of 58.1% with the lowest standard deviation (1.15%), indicating the most homogeneous pore distribution and the best dimensional stability. These findings provide a scientific basis that scaffolds based on green mussel shell waste and gelatin represent a viable and economical biomaterial alternative possessing physical equivalence to commercial products for bone regeneration applications. The contribution of this research lies in providing empirical data supporting the utilization of local waste as sustainable biomaterials, as well as mapping the relationship between gelatin concentration and scaffold porosity, which can serve as a reference for the future development of composite scaffolds.

REFERENCES

Akbari, S., & Khazaeinejad, P. (2025). Parametric Evaluation of 3D-Printed Polylactic Acid Scaffolds: Balancing Mechanical and Biological Performance for Bone Tissue Engineering. *Results in Engineering, 26*.

Arokiasamy, P., Al Bakri Abdullah, M. M., Abd Rahim, S. Z., Luhar, S., Sandu, A. V., Jamil, N. H., & Nabiałek, M. (2022). Synthesis Methods of Hydroxyapatite from Natural Sources: A Review. *Ceramics International, 48*(11), 14959–14979.

Charlena, Maddu, A., & Hidayat, T. (2022). Synthesis and Characterization of Hydroxyapatite From Green Mussel Shell With Sol-Gel Method. *Jurnal Kimia Valensi, 8*(2), 269–279.

Chinnasami, H., Dey, M. K., & Devireddy, R. (2023). Three-Dimensional Scaffolds for Bone Tissue Engineering. *Bioengineering, 10*(7).

Daskalakis, E., Iqbal, N., Loganathan, S., Spettoli, E., Morozzi, G., Ballardini, A., Giannoudis, P. V., & Jha, A. (2024). Effect of Laser Drilling on Biomorphically Engineered Hydroxyapatite Scaffolds Derived From Rattan Wood. *Materials and Design, 245*.

Dugaich, A. P. C., Barboza, A. S., Silva, M. G. E., Nörnberg, A. B., Maraschin, M., Badaró, M. M., Silva, D. F., Campos, C. E. M., Santinoni, C. S., Stolf, S. C., Lund, R. G., & Andrade, J. S. R. (2025). Sustainable Valorization of Mussel Shell Waste: Processing for Calcium Carbonate Recovery and Hydroxyapatite Production. *Journal of Functional Biomaterials, 17*(1), 24.

Fitriyana, D. F., Ismail, R., Bayuseno, A. P., Widodo, R. D., Rusiyanto, Anis, S., Siregar, J. P., & Cionita, T. (2024). Microwave Irradiation, Hydroxyapatite, Biological Sources, Sustainable Development Goals (SDGs).

González-Henríquez, C. M., Rodríguez-Umanzor, F. E., Acuña-Ruiz, N. F., Vera-Rojas, G. E., Terraza-Inostroza, C., Cohn-Inostroza, N. A., Utrera, A., Sarabia-Vallejos, M. A., & Rodríguez-Hernández, J. (2022). Fabrication and Testing of Multi-Hierarchical Porous Scaffolds Designed for Bone Regeneration via Additive Manufacturing Processes. *Polymers, 14*(19).

Gregor, A., Filová, E., Novák, M., Kronek, J., Chlup, H., Buzgo, M., Blahnová, V., Lukášová, V., Bartoš, M., Nečas, A., & Hošek, J. (2017). Designing of PLA Scaffolds for Bone Tissue Replacement Fabricated by Ordinary Commercial 3D Printer. *Journal of Biological Engineering, 11*(1).

Guagnini, B., Medagli, B., Zumbo, B., Cannillo, V., Turco, G., Porrelli, D., & Bellucci, D. (2024). Alginate-Sr/Mg Containing Bioactive Glass Scaffolds: The Characterization of a New 3D Composite for Bone Tissue Engineering. *Journal of Functional Biomaterials, 15*(7).

Ismail, R., Cionita, T., Lai, Y. L., Fitriyana, D. F., Siregar, J. P., Bayuseno, A. P., Nugraha, F. W., Muhamadin, R. C., Irawan, A. P., & Hadi, A. E. (2022). Characterization of PLA/PCL/Green Mussel Shells Hydroxyapatite (HA) Biocomposites Prepared by Chemical Blending Methods. *Materials, 15*(23).

Jiao, J., Hong, Q., Zhang, D., Wang, M., Tang, H., Yang, J., Qu, X., & Yue, B. (2023). Influence of Porosity on Osteogenesis, Bone Growth and Osteointegration in Trabecular Tantalum Scaffolds Fabricated by Additive Manufacturing. *Frontiers in Bioengineering and Biotechnology, 11*.

Kang, M., Lee, C. S., & Lee, M. (2021). Bioactive Scaffolds Integrated With Liposomal or Extracellular Vesicles for Bone Regeneration. *Bioengineering, 8*(10).

Lukin, I., Erezuma, I., Garcia-Garcia, P., Reyes, R., Evora, C., Kadumundi, F. B., Dolatshahi-Pirouz, A., & Orive, G. (2023). Sumecton Reinforced Gelatin-Based Scaffolds for Cell-Free Bone Regeneration. *International Journal of Biological Macromolecules, 249*.

Maji, K., Dasgupta, S., Kundu, B., & Bissoyi, A. (2015). Development of Gelatin-Chitosan-Hydroxyapatite Based Bioactive Bone Scaffold with Controlled Pore Size and Mechanical Strength. *Journal of Biomaterials Science, Polymer Edition, 26*(16), 1190–1209.

Naghavi, S. A., Tamaddon, M., Marghoub, A., Wang, K., Babamiri, B. B., Hazeli, K., Xu, W., Lu, X., Sun, C., Wang, L., Moazen, M., Wang, L., Li, D., & Liu, C. (2022). Mechanical Characterisation and Numerical Modelling of TPMS-Based Gyroid and Diamond Ti6Al4V Scaffolds for Bone Implants: An Integrated Approach for Translational Consideration. *Bioengineering, 9*(10).

Nawafi, M. R., Masruroh, M., & Santjojo, D. J. D. H. (2022). Morphological and Mechanical Study of Gelatin/Hydroxyapatite Composite Based Scaffolds for Bone Tissue Regeneration. *Indonesian Journal of Applied Physics, 12*(2), 235.

Peng, W., Liu, Y., & Wang, C. (2023). Definition, Measurement, and Function of Pore Structure Dimensions of Bioengineered Porous Bone Tissue Materials Based on Additive Manufacturing: A Review. *Frontiers in Bioengineering and Biotechnology, 10*.

Prasetyo, A., Bayuseno, A. P., Fitriyana, D. F., Anis, S., & Siregar, J. P. (2025). The Potential of Green Mussel Shells as a Source of Hydroxyapatite for Biomedical Applications: A Comparative Study with Commercial Hydroxyapatite. *20*(11).

Pratama, Y. A., Marhaeny, H. D., Deapsari, F., Budiatin, A. S., Rahmadi, M., Miatmoko, A., Taher, M., & Khotib, J. (2025). Development of Hydroxyapatite as a Bone Implant Biomaterial for Triggering Osteogenesis. *European Journal of Dentistry*.

Priyani, P. A., Fitriyana, D. F., Anis, S., Ismail, R., Prasetyo, A., Afrizal, M., Imran, A. I., Siregar, J. P., & Cionita, T. (2025). Pengaruh Daya Ultrasonik terhadap Karakterisasi Hidroksiapatit yang Disintesis dengan Metode Gelombang Mikro. *16*(2).

Shan, E., Chamorro, C., Ferrández-Montero, A., Martin-Rodriguez, R. M., Ferrari, B., Sanchez-Herencia, A. J., Virto, L., Marín, M. J., Figuero, E., & Sanz, M. (2025). In Vitro Biological Properties Assessment of 3D-Printed Hydroxyapatite–Polylactic Acid Scaffolds Intended for Bone Regeneration. *Journal of Functional Biomaterials, 16*(6).

Sun, J., Chen, C., Zhang, B., Yao, C., & Zhang, Y. (2025). Advances in 3D-Printed Scaffold Technologies for Bone Defect Repair: Materials, Biomechanics, and Clinical Prospects. *BioMedical Engineering Online, 24*(1).

Tseng, Y.-S., Chang, W.-H., Cheng, Y.-J., Wang, C.-K., & Chen, W.-F. (2024). Porous Hydroxyapatite Bioscaffolds via Hybrid FDM-DLP 3D Printing With Porogen Engineering. *International Journal of Clinical Medicine and Bioengineering, 4*, 1–10.

Wu, E., Huang, L., Shen, Y., Wei, Z., Li, Y., Wang, J., & Chen, Z. (2024). Application of Gelatin-Based Composites in Bone Tissue Engineering. *Heliyon, 10*(16), e36258.

Zhao, R., Yang, R., Cooper, P. R., Khurshid, Z., Shavandi, A., & Ratnayake, J. (2021). Bone Grafts and Substitutes in Dentistry: A Review of Current Trends and Developments. *Molecules, 26*(10).